

AN ABSTRACT OF THE THESIS OF

Nicki Perreault for the degree of Master of Science in Physics
presented on May 26, 1999. Title: Temperature Dependence of the
Photorefractive Effect in Doped Cadmium Fluoride.

Abstract approved:

Redacted for Privacy

William W. Warren

Holographic techniques were used to study the optical properties and bistable behavior of Ga-doped cadmium fluoride. Ga impurities form bistable centers in CdF_2 . Illumination causes a phototransformation from a deep to shallow center, which causes a change in the index of refraction. This change is caused by a redistribution of electrons in the centers, and is known as the photorefractive effect.

The photorefractive effect makes it possible to write holographic patterns into the material. Using intersecting laser beams, a holographic grating was written into the sample, and the behavior of this grating was studied. The decay and efficiency of the grating are temperature dependent. The thermal decay that is responsible for

erasing the grating is a two-center process. The thermal activation energy between the centers is about 780 meV.

Temperature Dependence of the Photorefractive Effect in Doped
Cadmium Fluoride

by

Nicki Perreault

A THESIS

submitted to

Oregon State University

in partial fulfillment of
the requirements for the
degree of

Master of Science

Presented May 26, 1999
Commencement June 2000

Master of Science thesis of Nicki Perreault presented on May 26, 1999

APPROVED:

Redacted for Privacy

Major Professor, representing Physics

Redacted for Privacy

~~Chair of~~ Department of Physics

Redacted for Privacy

Dean of Graduate School

I understand that my thesis will become part of the permanent collection of Oregon State University libraries. My signature below authorizes release of my thesis to any reader upon request.

Redacted for Privacy

Nicki Perreault, Author

ACKNOWLEDGEMENTS

There are many people who have helped me tremendously in completing this thesis. Although it is not possible to mention them all here, I would like to recognize those who deserve a special thank you.

First, I would like to thank my adviser, Dr. Bill Warren. Without his guidance and encouragement, this work could not have been completed. I would also like to thank Mark Shroyer for all his help, and for patiently answering an endless stream of questions. Dr. David McIntyre and Tim Taylor have been very generous with both their time and their equipment.

I would also like to acknowledge Alexei Ryskin of the Vasilov State Optical Institute in St. Petersburg, Russia, for providing the samples for this research.

Finally, I have been fortunate to have the love and support of my family and friends. I am grateful to my parents, my daughter Sammi, and my dear friends Tony and Jeff for their inspiration and encouragement.

TABLE OF CONTENTS

	<u>Page</u>
1. INTRODUCTION	1
1.1 Observed Behaviors in CdF_2	1
1.2 Outline of Experiment	2
2. REVIEW OF LITERATURE	5
2.1 Experimental Data	5
2.2 Current Theoretical Model.....	10
3. EXPERIMENTAL METHOD.....	17
3.1 The Sample.....	17
3.2 The Writing Process.....	17
3.3 The Reading Process.....	21
3.4 The Measurements.....	27
4. RESULTS AND ANALYSIS.....	28
4.1 Laser Power and Grating Efficiency.....	28
4.2 Temperature and Grating Efficiency.....	30
4.3 Relaxation Times and Activation Energy.....	32
5. CONCLUSIONS.....	38
BIBLIOGRAPHY.....	40

LIST OF FIGURES

<u>Figure</u>	<u>Page</u>
2.1 Absorption spectrum of CdF ₂ :Ga at 10 K	6
2.2 Absorption spectrum of CdF ₂ :In before (1) and after (2) illumination	7
2.3 Cadmium fluoride lattice structure	11
2.4 Formation of DX center in CdF ₂ :Ga	13
2.5 Electronic charge density contours	14
2.6 Configuration diagram for metastable center in CdF ₂	15
3.1 Interference pattern created by intersecting beams of coherent light	18
3.2 Diagram of writing equipment	20
3.3 The Mach-Zehnder interferometer	22
3.4 Boxcar sampling points	25
3.5 Diagram of recording equipment	26
4.1 Laser power and grating efficiency	29
4.2 Temperature and grating efficiency	31
4.3 Decay of shallow center at 293 K	35
4.4 Decay of shallow center at 308 K	36
4.5 Activation energy	37

TEMPERATURE DEPENDENCE OF THE PHOTOREFRACTIVE EFFECT IN DOPED CADMIUM FLUORIDE

1. INTRODUCTION

1.1 Observed Behaviors in CdF₂

Cadmium fluoride is a material that exhibits interesting bistable behavior when doped with gallium or indium. For example, the optical absorption spectrum of CdF₂:Ga has two broad bands. One is in the visible range, and the other is in the infrared region. If the material is cooled in the dark below a certain temperature, the only band seen is the absorption in the visible range. Illumination with white light causes absorption in the visible band to decrease while that of the infrared increases. At sufficiently low temperatures, this change in absorption persists even after the light source is removed. This behavior suggests a change from a lower to a higher energy state under illumination. The metastability of this transformation has led to suggestions that electrons are somehow trapped in a shallow energy state at low temperatures.

The material also undergoes a change in the index of refraction under illumination with white light. This behavior is referred to as the photorefractive effect. In CdF₂:Ga the photorefractive effect is

localized in regions of high light intensity and metastable below a certain critical temperature. Illumination of one portion of the crystal causes a change in the index of refraction in just that portion, and at low temperatures this effect persists after the light source is removed.

The photorefractive effect makes it possible to write holographic patterns into this material. In Ga-doped CdF_2 , the temperature at which the effect is metastable is above 200 K [1], which is very high for this type of material. For example, In-doped CdF_2 and other materials of this class have metastable effects at or below 100 K [1]. Because of the high temperature observed in Ga-doped CdF_2 , this material could be a possible candidate for storing high-density optical data. It seems worthwhile to study the mechanisms responsible for the photorefractive effect in $\text{CdF}_2\text{:Ga}$.

Other photo-induced metastable effects include persistent photoconductivity [2], photo-induced lattice shrinkage [3], and photo-magnetism [4].

1.2 Outline of Experiment

Based on the observed behaviors, Ga donors are thought to form bistable centers in CdF_2 crystals [2]. This idea will be explored in detail in the following chapter. The exact mechanisms responsible for the changes in absorption and the photorefractive effect are not

fully understood. The goal of this experiment was to try to gain an understanding of the dynamics of the processes involved in the photorefractive effect. Using holographic techniques, a phase grating was written into the material. The temperature dependence of the grating and the effects of laser beam intensity were studied. These results provided information that was used to test the currently accepted theoretical model for this material. Specifically, the efficiency of the grating was measured as the holographic interference pattern was varied. The efficiency is a measure of the degree to which the index of refraction was changed by the holographic pattern. Because this change is directly related to the population of the shallow centers, measurements of the efficiency can be used to analyze the behavior of this shallow state. These measurements were made over a wide range of temperatures, as well as over a range of writing intensities. There is believed to be an energy barrier between the two configurations of the bistable centers in CdF_2 that is responsible for the metastable behavior of the photorefractive effect[2]. This experiment provided the temperature dependence of the decay of the shallow center, which allowed a direct calculation of the proposed energy barrier.

These results will be used in conjunction with NMR studies currently being conducted independently on the same material to

help understand the microscopic mechanisms involved in the photorefractive effect. The optical studies can determine the energy barrier and gain information about the photoionization energy needed for the photorefractive effect. This information cannot be determined by NMR studies alone, so the results of this experiment should help clarify the findings of NMR studies. By studying this material both optically and magnetically, it should be possible to gain an accurate picture of the mechanisms involved in the photorefractive effect in Ga-doped CdF_2 .

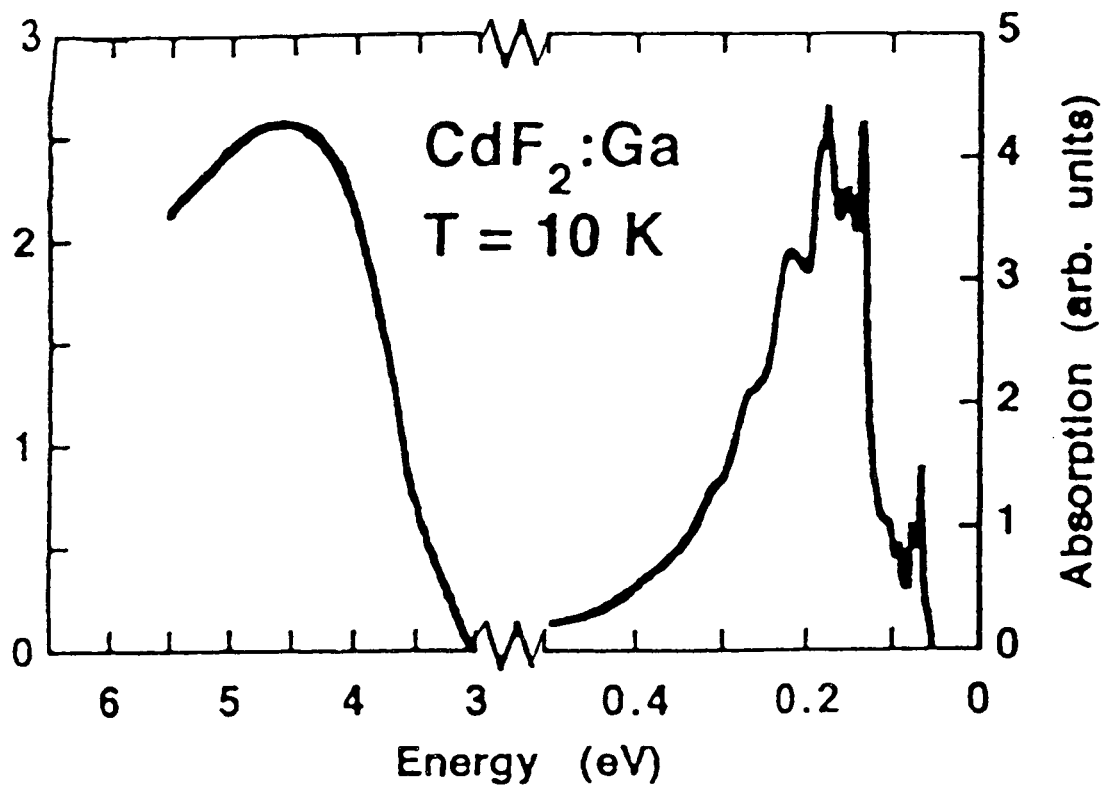
2. REVIEW OF LITERATURE

The following is a review of previous experimental results on this material. This is followed by the currently accepted theoretical model of Ga and In defects in CdF_2 .

2.1 Experimental Data

Previous experimental work on optical bistability and metastability has been done on both Ga- and In-doped CdF_2 . The absorption spectrum of $\text{CdF}_2\text{:Ga}$ has two broad bands [1]. One is centered on 4.5 eV in the UV/VIS range, and the other is centered on 0.2 eV in the infrared range (Figure 2.1) [1]. If the crystal is cooled in the dark below some critical temperature, only the higher energy band is present. Illumination causes the low energy absorption band to grow, while the high energy one is bleached. Figure 2.2 shows the absorption of $\text{CdF}_2\text{:In}$ cooled to 5 K in the dark (solid line) and after illumination (dashed line) [5]. This change in absorption persists after the light source is removed, provided the temperature is low enough. Accompanying this change in absorption is a metastable change in the index of refraction, and the appearance of persistent photoconductivity. The change in refractive index is 10^{-3} to 10^{-4} for wavelengths of 0.5 to 1.5 μm and doping concentrations of

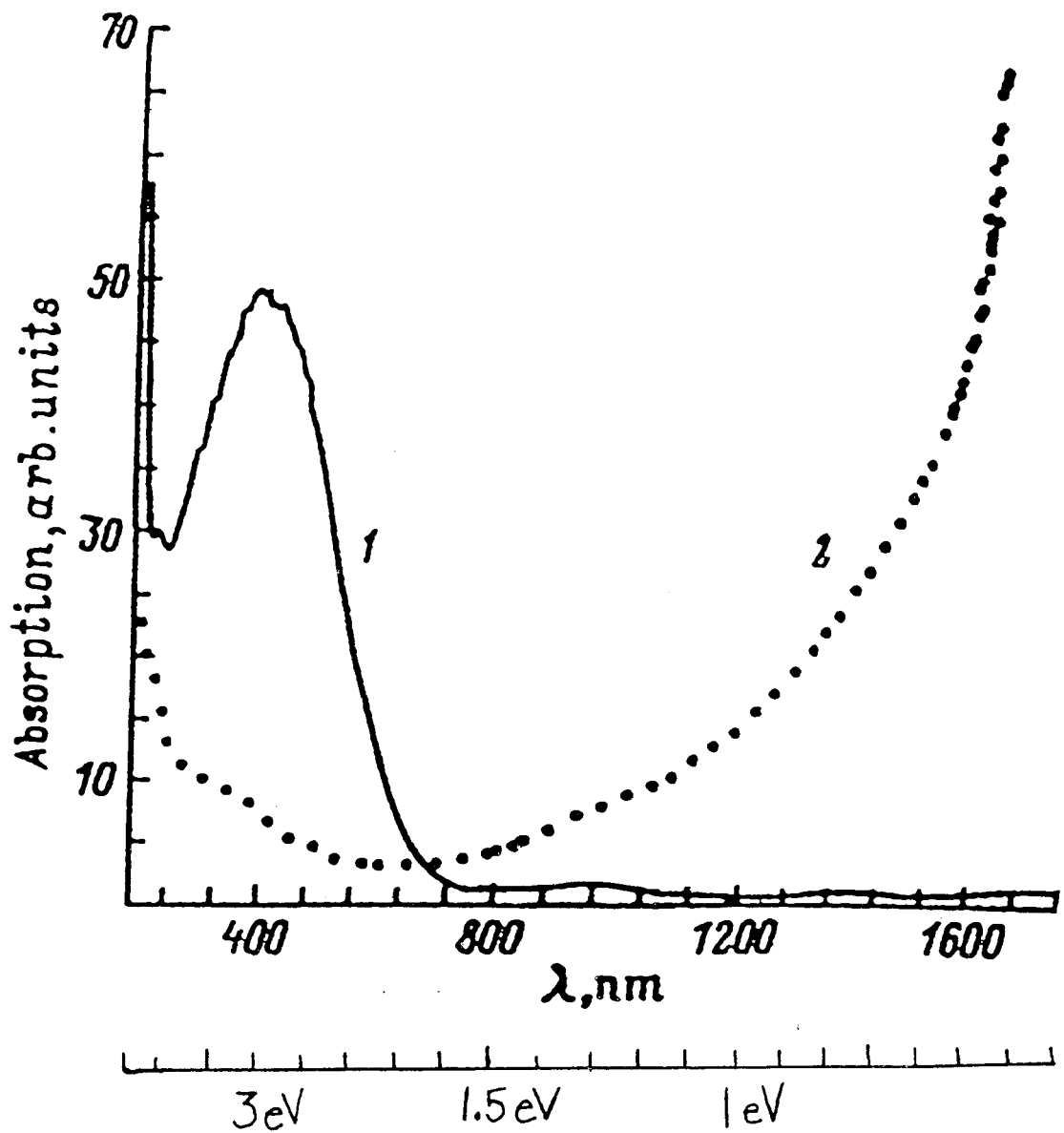
FIG 2.1 Absorption spectrum of $\text{CdF}_2:\text{Ga}$ at 10 K



Suchoki *et al.*, 1997

FIG 2.2 Absorption spectrum of $\text{CdF}_2:\text{In}$ before (1) and after (2) illumination

Ryskin, 1997



10^{17} cm^{-3} [1]. Much of the previous work done on this material has led to the idea that the deep state is a DX center. DX centers are formed when a neutral donor impurity traps an additional electron and shifts to an off-lattice site. In a DX center, the effective Hubbard correlation energy, U , is negative. This is because the electrostatic repulsion between the two electrons is overcompensated by the lattice energy gained in the distortion. There are a variety of experimental methods that have shown the negative U nature of the deeper state. Experiments on the paramagnetic susceptibility of $\text{CdF}_2:\text{In}$ showed that paramagnetism is present in the shallow center, but it is absent in the deep center[6]. Photoelectron paramagnetic resonance studies showed an absence of a paramagnetic moment in the deep state[7]. Also, analysis of shallow-deep kinetics in both In- and Ga-doped samples showed a quantum yield of two electrons per photon for transitions between centers[8]. This indicates that the deep state is a negative- U center with two electrons, and the shallow center has just one electron.

There is also evidence that there are not just one, but two DX centers in $\text{CdF}_2:\text{Ga}$ [16]. Analysis of the thermal and optical transitions showed that there are three states for the Ga center. One of these is a one-electron, shallow center, and the other two are deep negative- U states. For samples with high doping concentrations

(greater than $N_{\text{Ga}} = 1.5 \times 10^{17} \text{ cm}^{-3}$), the formation of the second DX center is strongly suppressed.

Experimental data indicate a lattice relaxation associated with the deep center. The Stokes shift, which is a measure of the difference in the thermal and optical energy levels, is very large [9]. In In-doped samples, it is 1.8 eV. A Stokes shift of this magnitude is indicative of a large difference in the localization of the deep and shallow centers. Also in In-doped samples, Suchoki *et al.* [3] measured the differential photo-induced lattice dilation using a scanning tunneling microscope. The change in the lattice constant during phototransformation of the bistable centers is $(\Delta a/a) = 1.8 \times 10^{-6}$. Another experimental method that implies an asymmetric lattice relaxation is work done recently on both Ga- and In-doped crystals using positron annihilation [10]. These experiments revealed an open-volume defect that is at least half of a Cd monovacancy. These results suggest a bond breaking mechanism, resulting in asymmetric lattice relaxations during phototransformation.

Holographic patterns have been studied in both Ga- and In-doped crystals. Ryskin *et al.* [11] and Langer *et al.* [1] have studied the sensitivity and decay of gratings in $\text{CdF}_2\text{:Ga}$. They report grating efficiencies of greater than 20% for writing temperatures up to 400 K. Diffraction efficiency and decay times are temperature dependent

with a maximum efficiency occurring at 260-280 K, and metastable effects below 250 K. They measured the thermal decay time of the grating, and fit the initial part of the decay to an exponential. Using this method, they found the activation energy to be 650 meV for temperatures between 285 and 333 K.

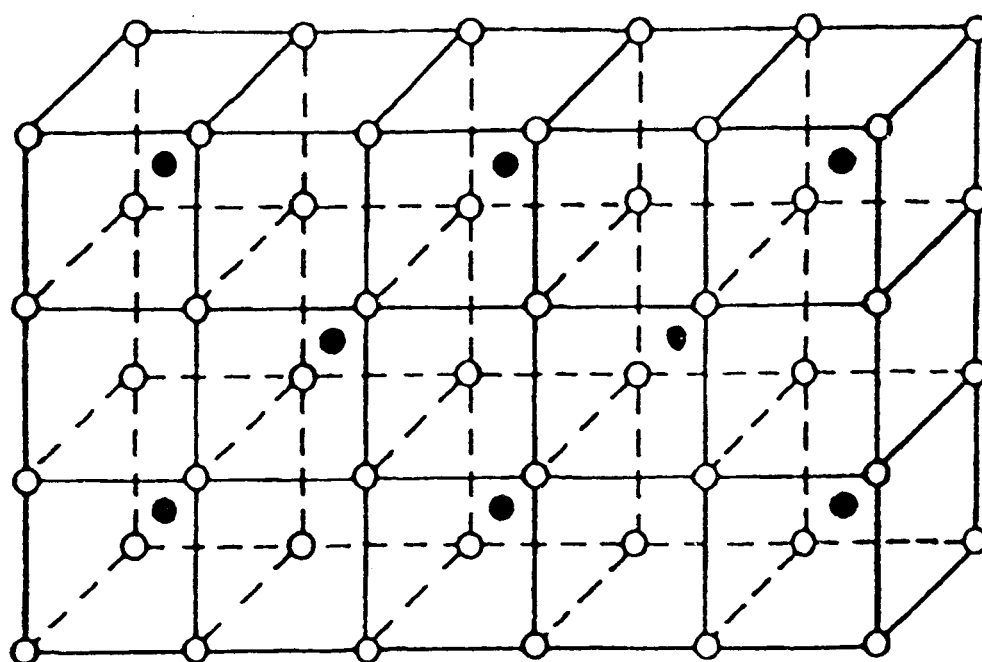
In similar studies on $\text{CdF}_2:\text{In}$, the maximum grating efficiency occurs at 100 K and the thermal energy barrier is 200 meV [12].

2.2 Current Theoretical Model

In CdF_2 crystals, the F atoms form a simple cubic sublattice. Cd atoms are located at the centers of alternate F cubes so half the cubes have a Cd at the center. Each F is tetrahedrally bonded to four Cd atoms, while each Cd is bonded to eight F atoms (See Figure 2.3). The band gap is about 7.8 eV, and the lattice constant is 2.677 \AA [2]. When CdF_2 is doped with Ga, the Ga donor atom takes the place of a Cd at the center of an F cube.

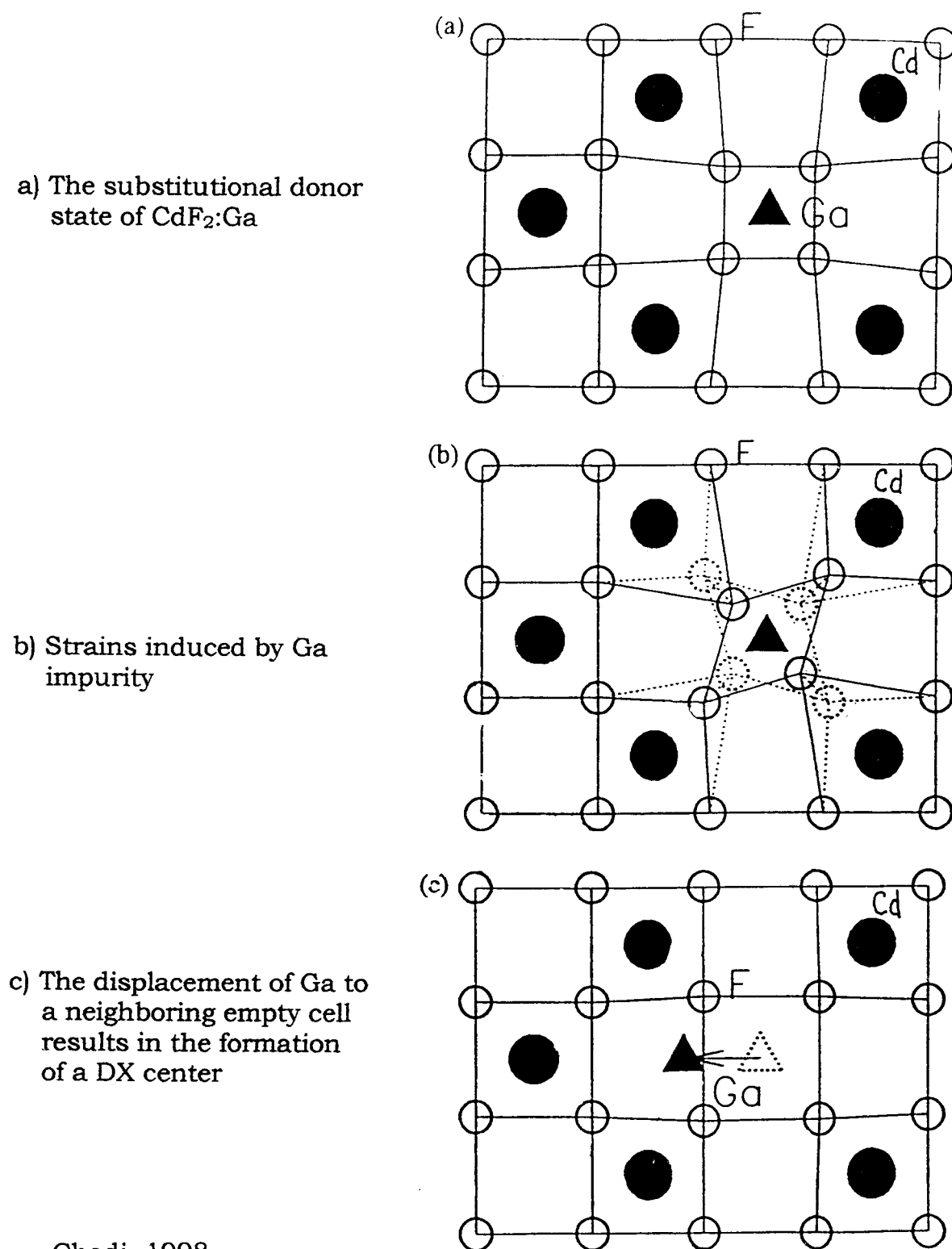
Ga is believed to form bistable centers in this material. This means that electrons are trapped either at a deep, localized state, or in a shallower hydrogen-like state. Recent theoretical work by C.H.Park and D.J.Chadi [2] proposes that the ground state of this material has two electrons and consists of Ga^{1+} and Ga^{3+} . The shallow state is believed to have one electron, and consists of Ga^{3+}

FIG 2.3 Cadmium fluoride lattice structure



and a bound electron. It would seem impossible for the two-electron center to have a lower energy than that of the one-electron center, because of the repulsion forces present. However, the ground state is thought to be a DX center, with the donor impurity undergoing a large lattice relaxation, thereby lowering the energy[2]. The smaller ionic radius of Ga compared to Cd introduces a strain on the lattice, raising the energy (See Figure 2.4). The Ga donor then undergoes a lattice relaxation and moves into a nearby empty cube of F atoms. From first principles calculations, this configuration is found to be stable in a negative charge state for Ga and In donors, with a displacement of 1.82 Å for the Ga-doped model. Applying the same calculations to Al or Sc donor impurities did not show the same lattice instabilities. Studies of the electron charge densities (Figure 2.5) show that changing the charge of the DX state makes this configuration unstable, and the Ga donor returns to the expected substitutional position for the shallow center.

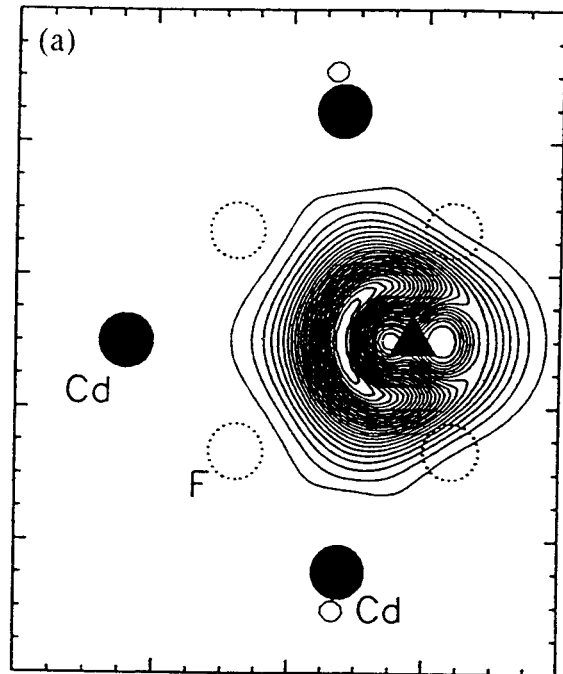
This type of model is often explained using a configuration coordinate sketch (See Figure 2.6)[5]. The energy is plotted as a function of some spatial coordinate, which is left unspecified. The ground state is represented by the lower parabola and is spatially shifted from the center represented by the upper parabola. Illumination causes a transformation (labeled E_{opt}) from the lower

FIG 2.4 Formation of DX center in $\text{CdF}_2:\text{Ga}$ 

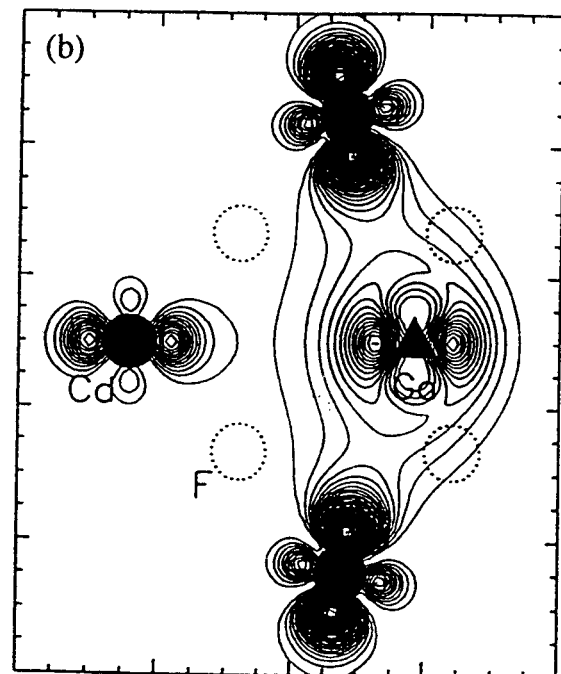
Chadi, 1998

FIG 2.5 Electronic charge density contours

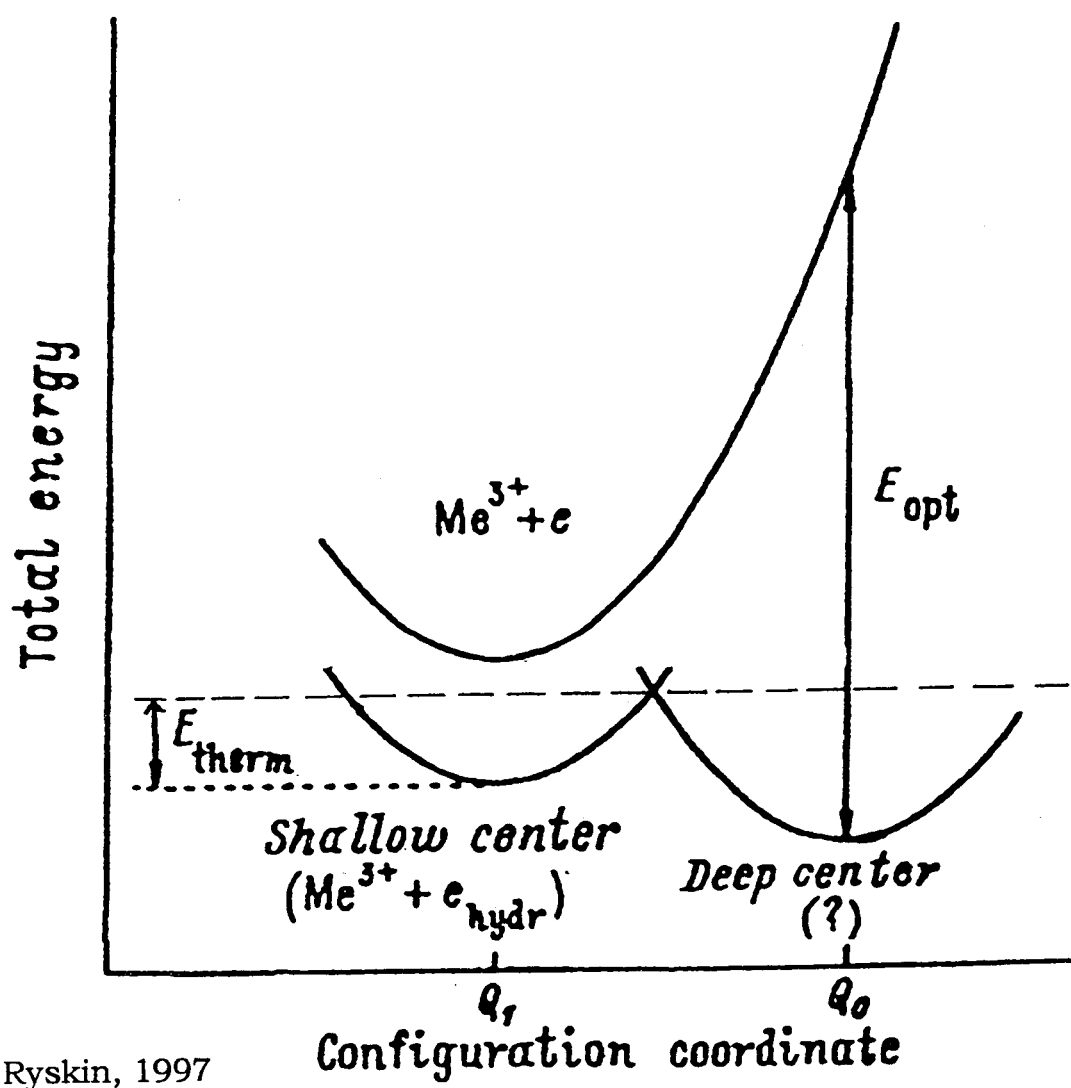
a) The deep donor state Ga:DX lying in the band gap



b) An occupied localized state showing the interaction between Cd-*d* and Ga-*d* orbitals

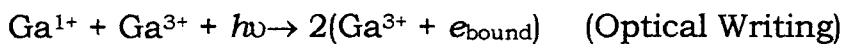


Chadi, 1998

FIG 2.6 Configuration diagram for metastable center in CdF_2 

parabola to the conduction band. Once there, the electron will undergo a lattice shift and relax into the upper parabola.

Photoionization of one deep center results in the formation of two shallow centers. During this process, a change in polarization occurs, which causes a change in the index of refraction. The photoionization from the ground state is often referred to as the writing process. For the electrons to decay from the shallow center, two things must happen. First, the electron must possess the thermal energy needed to overcome the barrier between the parabolas. This energy is referred to as the activation energy of the shallow center. Second, the electron must be able to pair with another electron to decay into the ground state. This relaxation reverses the change in the index of refraction, and is called the erasing process. These processes obey the equations:



Theoretical calculations predict that the thermal energy barrier, kT , is on the order of 1 eV for Ga-doped crystals [2]. Experimental measurements of the photoionization energy, $\hbar\omega$, are ~2.5 eV for In-doped and ~3.7 eV for Ga-doped [5].

3. EXPERIMENTAL METHOD

3.1 The Sample

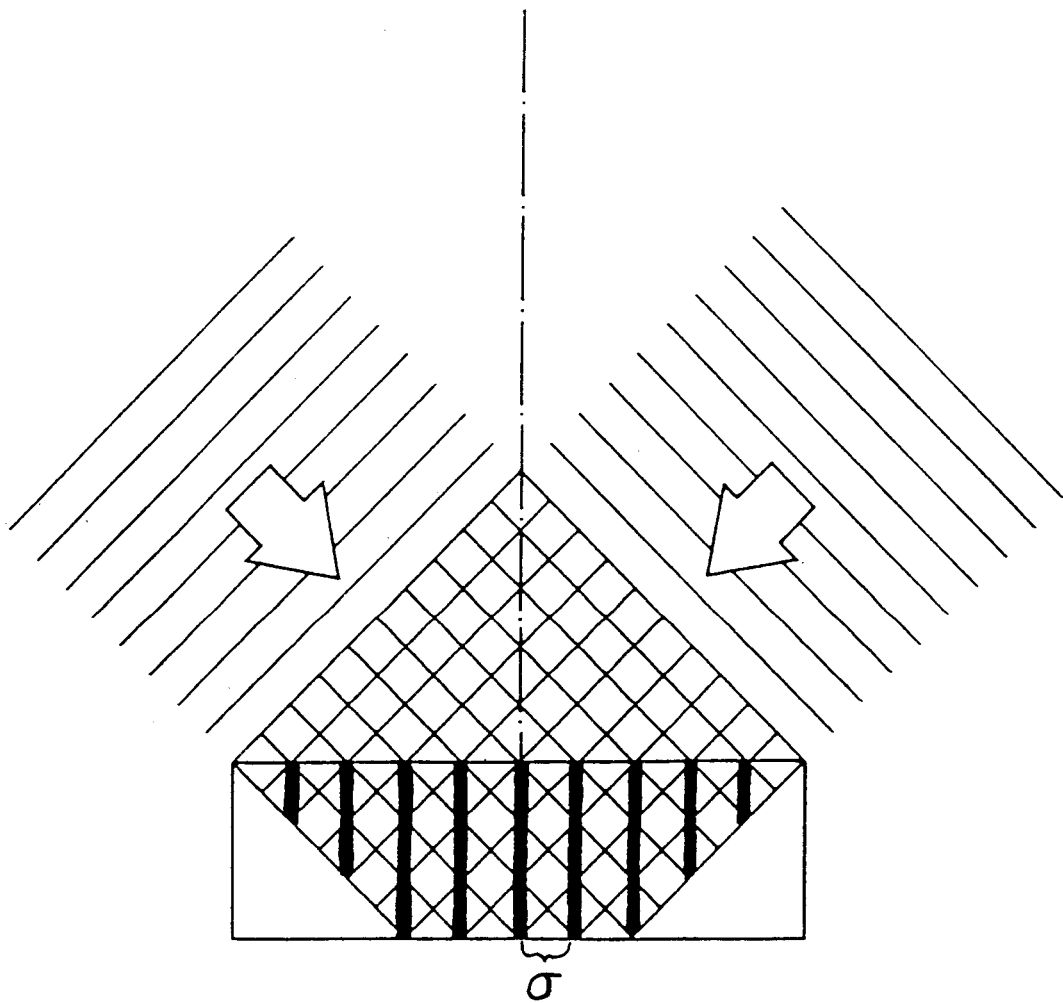
The sample used in this experiment was an unpolished CdF_2 crystal doped with Ga. The doping concentration was on the order of 10^{18} cm^{-3} . The dimensions of the crystal were 0.6 mm x 0.5 mm x 0.2 mm. Alexei Ryskin of the Vasilov State Optical Institute in St. Petersburg, Russia, supplied the crystals.

3.2 The Writing Process

3.2.1 Holographic Gratings

Two coherent, intersecting beams of light create an interference pattern with regions of high and low intensities (See Figure 3.1). In standard holography, photographic film is exposed to this type of interference pattern and a hologram is recorded. In this experiment, exposing the sample to the three-dimensional interference pattern creates a volume hologram. In the regions of high intensity, electrons are excited into the shallow hydrogenic state, thereby changing the index of refraction. In the dark regions, if the interfering beams are of equal intensity, the electrons are unaffected and remain in the DX center. Because the photorefractive effect is highly localized, the change in index of refraction is limited to the high intensity regions in

FIG 3.1 Interference pattern created by intersecting beams of coherent light



the interference pattern. The result is a three-dimensional holographic grating written into the sample. The wavelength and angle between writing beams determine the grating constant. According to Bragg's Law, the grating constant, or spacing between fringes in the interference pattern, is

$$\sigma = \frac{\lambda}{2 \sin \theta}$$

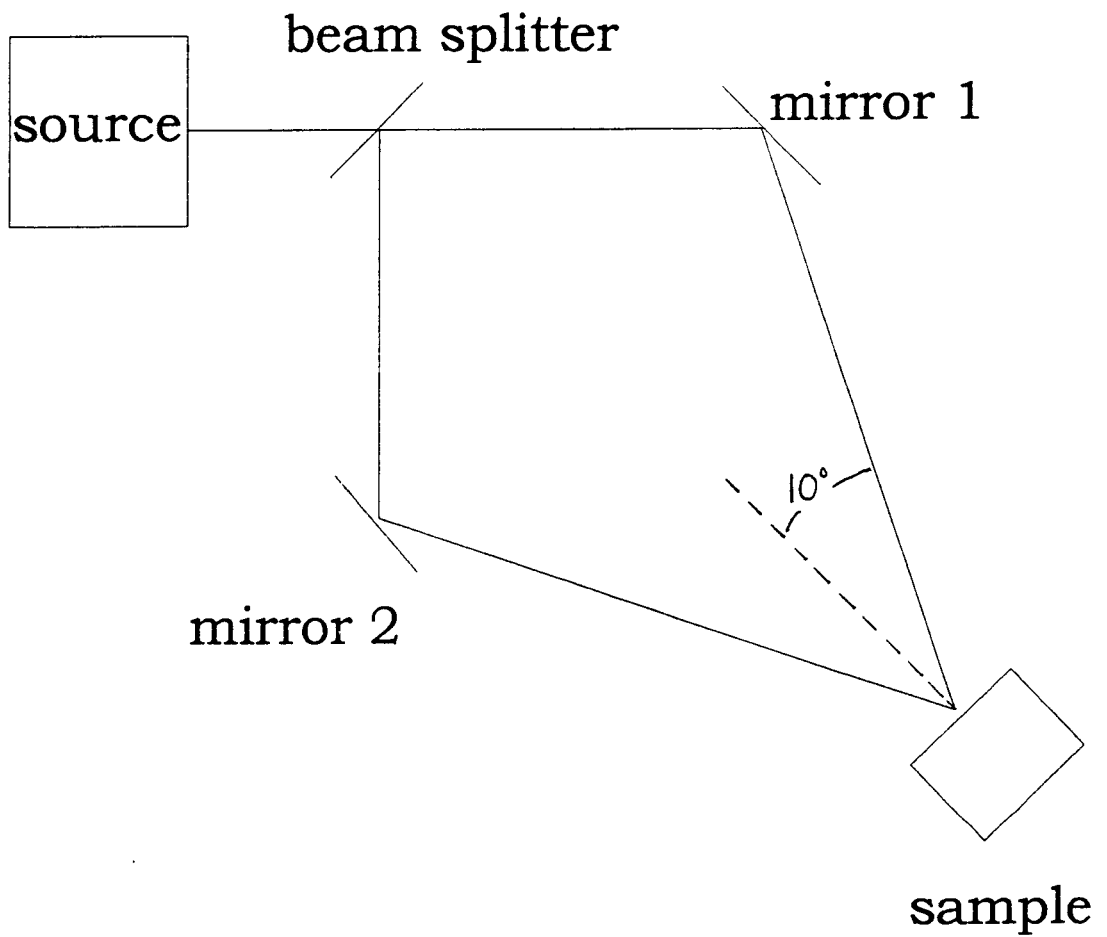
3.2.2 Equipment

The grating was written using a Coherent Innova 300 Argon Ion Laser with a wavelength of 465 nm, operating at power levels below 30 mW. The CdF₂ crystal was placed in an optical Joule-Thompson refrigerator from MMR [14] which has a temperature range from 80 K to 373 K. The sample was affixed to the cold stage using copper foil and thermal grease, and kept under a vacuum of 10⁻³ torr.

3.2.3 The Writing Set-up

To write the grating into the sample, the beam was sent through a beam splitter, and both beams were balanced to within 3%. The beams were then focused onto the sample with both beams at an angle of 10 degrees from the normal (See Figure 3.2). This resulted in a grating constant of 1.3 μm for a writing wavelength of 465 nm.

FIG 3.2 Diagram of writing equipment

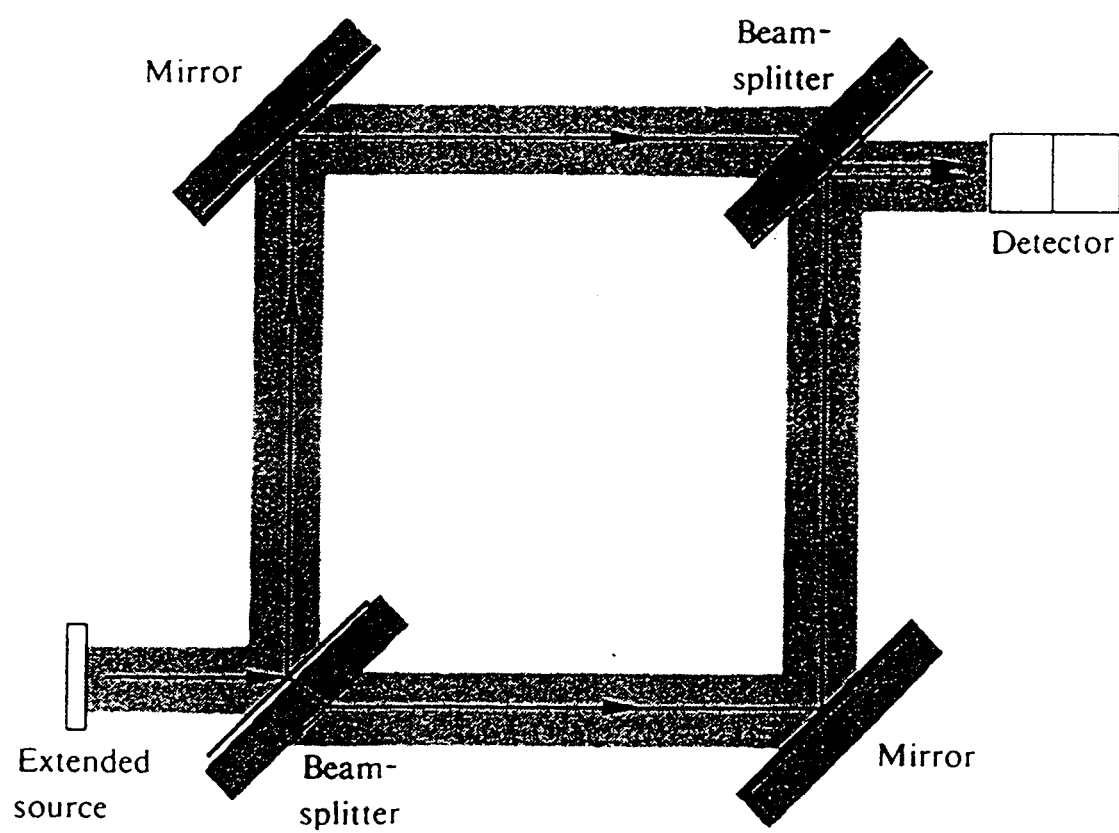


3.3 The Reading Process

3.3.1 The Mach-Zehnder Interferometer

The Mach-Zehnder interferometer is a variation of the well-known Michelson interferometer. It consists of two beam splitters and two mirrors (See Figure 3.3)[15]. Fringe patterns are caused by the interference of the beams at the second beam splitter, and can be seen at the position of the detector. Any change in the path length of one of the beams causes this fringe pattern to shift. The writing procedure described in the previous section is essentially a Mach-Zehnder interferometer, with the sample taking the place of the second beam splitter. Once the grating is written into the sample, the regions of differing indices of refraction split the incident beam into reflected and refracted portions. The portion of the writing beam that is reflected depends upon the degree to which the index of refraction has been changed by the illumination. The efficiency of the grating can be determined by measuring the ratio of the reflected incident beam to the total incident beam.

FIG 3.3 The Mach-Zehnder interferometer



Hecht, 1987

3.3.2 Equipment and Technique

Using the principle of the Mach-Zehnder interferometer, the efficiency of the grating was determined by varying the position of one of the mirrors. This caused the path length of one of the writing beams to fluctuate, which changed the fringe pattern created by the sample. Two photo-diode detectors were placed behind the sample to read the light that was transmitted through the sample by each beam. The detectors used were high-speed silicon PIN photo-diodes from Thorlabs. They have a rise time of 20 ns and an active area of 13 mm². The detectors were placed at a distance of 3-6 cm behind the sample. All outside light sources were eliminated to reduce both background noise in the detectors and photoexcitation of the sample.

One of the writing mirrors was mounted on a piezo modulator, which caused the mirror to oscillate and changed the path length of the writing beam. A Hewlett Packard frequency generator, using a sine waveform with a frequency of 330 Hz, triggered the piezo modulator. This vibration in the writing beam caused the fringe pattern to shift. The detectors saw this shift as an oscillation in the intensity of light transmitted through the sample. These oscillations corresponded to light and dark fringes moving past the detector, and the amplitude of the oscillations gave a relative efficiency that could

be used to characterize the actual efficiency of the grating.

Because the actual efficiency is more difficult to measure, the relative efficiency (or amplitude of oscillations) was used for further measurements.

To quantitatively measure this amplitude, an EG&G Boxcar Integrator was used to record the voltage read by the detector at the maximum and minimum points in the oscillation. Figure 3.4 shows what was seen by the detector on an oscilloscope, as well as the points that the boxcar sampled. The boxcar sampled and averaged this amplitude with a sampling time constant of 10 μ s, and was externally triggered by the HP frequency generator. This averaged amplitude was then collected by a Data Precision signal digitizing and storage device, the Data 6000, where it could be stored as a function of time and accumulated over several sweeps to help reduce the effects of background noise (see Figure 3.5).

To characterize the relaxation time for the shallow state, one of the writing beams was blocked, allowing the other beam to uniformly illuminate the sample. After a time sufficient for the sample to reach a steady state (10 to 15 seconds for the laser writing power at 12 mW), the second beam was turned on. Different regions of the sample then experienced varying intensities in illumination due to the interference pattern of the beams, and the relaxation time could be found by

FIG 3.4 Boxcar sampling points

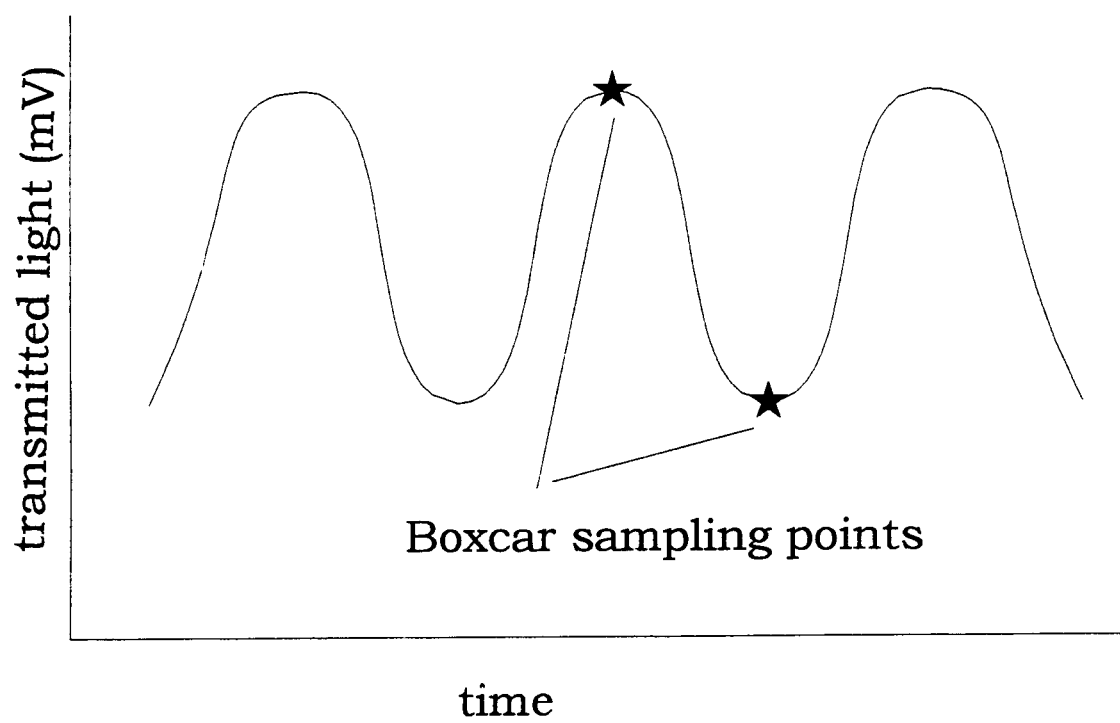
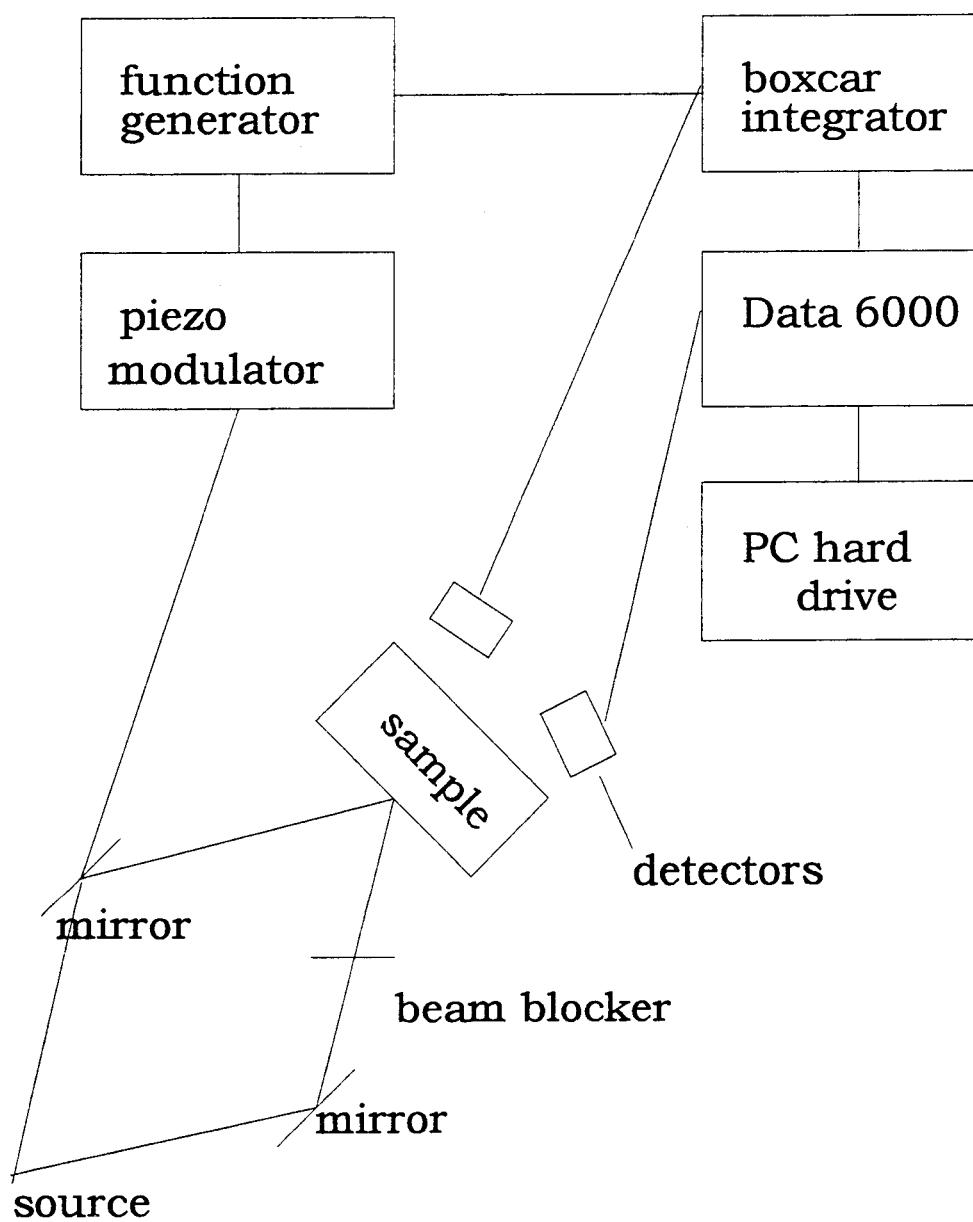


FIG 3.5 Diagram of recording equipment



observing the behavior of the amplitude of oscillations caused by the oscillating writing beam. The Data 6000 was triggered to start acquiring data when the second beam was turned on, and the changes in the amplitude of oscillations were recorded as a function of time. This was repeated and averaged over several trials to reduce the effects of noise in the data. Each trial sampled 256 data points with a sampling interval between 50 and 100 ms. Longer sampling intervals were needed for the cooler temperatures, where the time required for the relative efficiency to reach a maximum was longer.

3.4 The Measurements

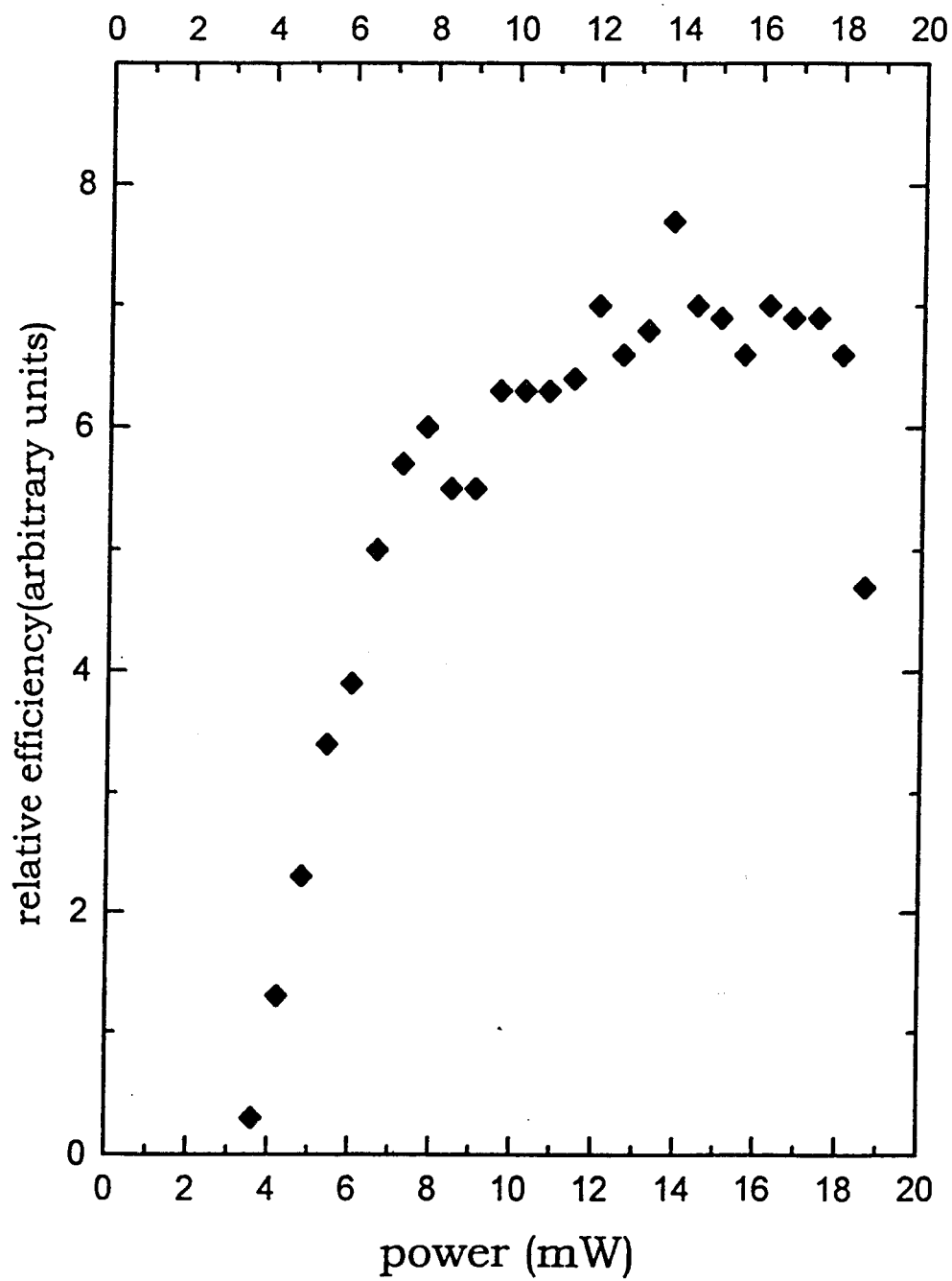
The procedure described above was used to measure the efficiency of the grating and the decay of the shallow state at various temperatures. Both properties were measured at 5-degree intervals in the temperature range from 240 K to 328 K. This procedure was not effective at temperatures outside this range, for reasons that will be discussed in the following section. The sample was allowed to come to equilibrium with the refrigerator temperature for ten to fifteen minutes between each measurement, and each measurement was repeated and averaged over eight to sixteen trials. In addition, the efficiency was measured at room temperature for laser output power between 3 and 18 mW.

4. RESULTS AND ANALYSIS

4.1 Laser Power and Grating Efficiency

The relative efficiency of the grating was measured for laser writing power between 3 and 18 mW at room temperature. The efficiency reached a maximum at 14 mW, and decreased at higher and lower beam power (See Figure 4.1). This is due to the two competing mechanisms in this material. One mechanism is the light causing photoionization from the DX center to the shallow center, and the other mechanism is the thermal decay of the shallow center. At very low writing power, the thermal decay rate is much faster than the rate of photoionization. As the intensity of light is increased, the photoionization rate increases, causing the efficiency to increase as well. However, as the power is increased beyond about 17 mW, the efficiency falls off rapidly. Here, the thermal decay rate increases because the increased beam power heats the sample. No measurements were attempted at beam strengths above 19 mW to avoid damage to the sample. All further measurements were made with the writing power between 10 and 12 mW. In this region, the efficiency is near maximum, but there is no danger of overheating the sample.

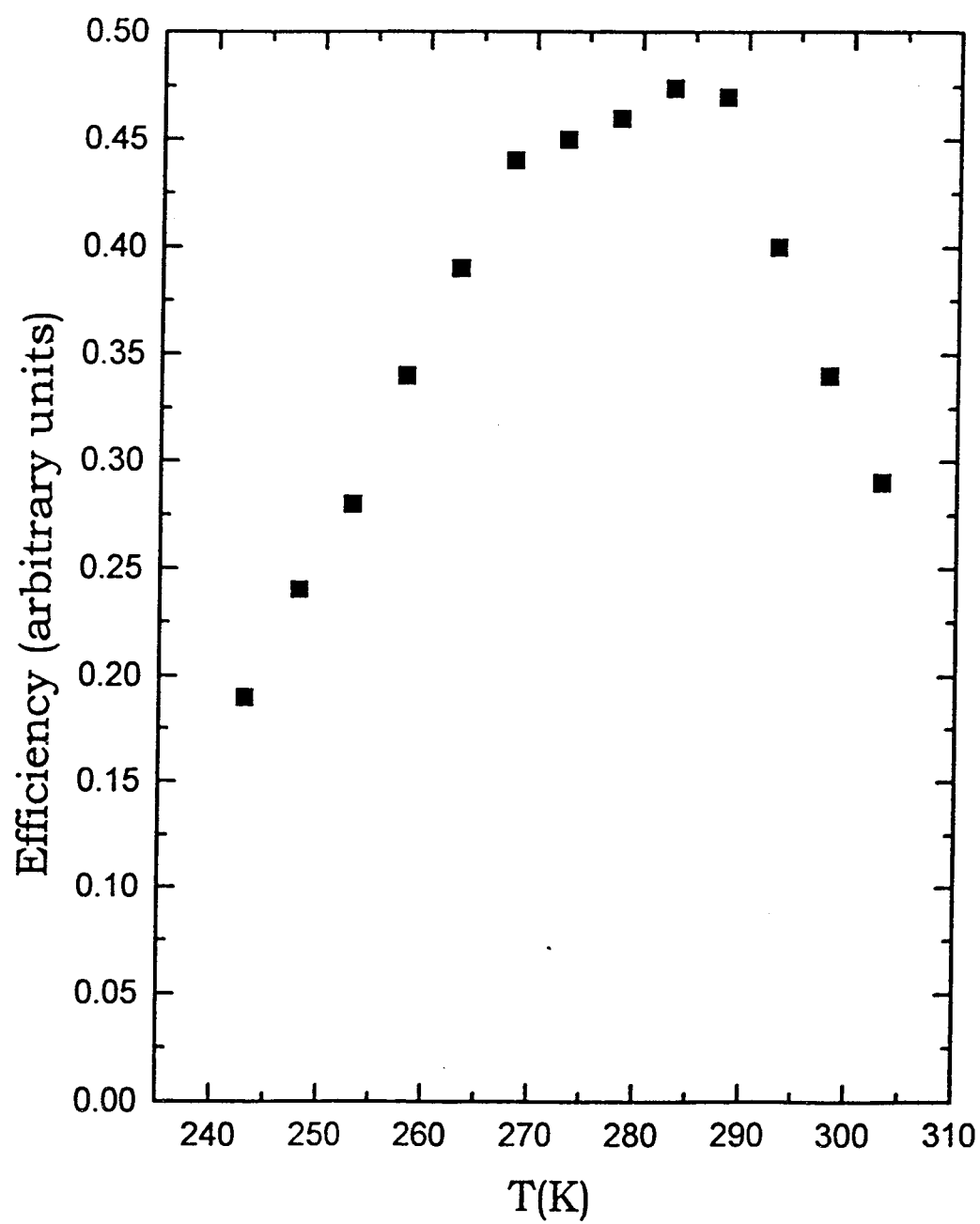
FIG 4.1 Laser power and grating efficiency



4.2 Temperature and Grating Efficiency

The relative efficiency of the grating was measured at 5-degree intervals between 240 K and 305 K. The efficiency reached a maximum at 285 K and decreased at higher and lower temperatures (See Figure 4.2). Again, this is due to the two competing mechanisms, but in a slightly different way than the previous measurement. At high temperatures, the thermal decay rate is too rapid for the index of refraction to be effectively changed by the interference pattern. At high temperatures, the high intensity regions of the interference pattern fail to change the index of refraction. On the other hand, at lower temperatures the electrons tend to be stuck in the shallow centers. In this case, the dark regions of the interference pattern are ineffective. At low temperatures, the amount of thermal energy available is small, causing the rate of thermal decay to be quite slow. Any stray light in the dark regions of the interference pattern causes a transformation from the DX center to the shallow center, and the lack of thermal energy traps the electron there. Stray light comes from imperfectly balanced beams and reflections from the cryostat surfaces, and is difficult to eliminate. At temperatures outside the range of this measurement, the grating efficiency was too small to provide any useful information. This

FIG 4.2 Temperature and grating efficiency



information determined the range of temperatures over which this experimental technique is effective.

4.3 Relaxation Times and Activation Energy

4.3.1 Decay Curves

The sample was uniformly illuminated with one beam for 20-30 seconds, and then the second beam was turned on. The amplitude of oscillations of the transmitted light increased as shallow centers in the dark regions of the interference pattern relaxed. This amplitude was recorded as a function of time, from the point when the second beam was turned on, for temperatures between 240 K and 328 K. At high temperatures, above 300 K, this amplitude reaches a maximum rapidly, because the shallow centers can readily acquire the thermal energy needed to relax.

At lower temperatures, the amplitude reaches its maximum much more slowly, and this maximum decreases substantially for temperatures below 250 K. As previously mentioned, the interference pattern cannot effectively write the grating at temperatures close to the onset of metastability. In this temperature range, the amplitude is too small to be distinguished from the background noise, and no longer gives any useful information about the relaxation times of the shallow centers.

4.3.2 Curve Fitting Models

To analyze the decay curves, it is necessary to fit them to a model that will correctly characterize the decay rate or relaxation times according to the physical processes involved. Although the curves appear to be exponential, the decay is believed to be a two-center process. If this were correct, the exponential model would be an inappropriate description of the decay. In an exponential decay, the probability for one state to decay is independent of the initial concentration and the behavior of other states. In a two-center process, the decay depends both on the thermal energy of the electron and the availability of another electron to pair with. Because the mechanisms are not fully understood, the data were analyzed using both a two-center model and an exponential model for comparison.

The model used to characterize the two-center process was the non-geminate recombination model. This type of model is often used to describe second-order chemical reactions (See ref. 13 for an example of this model). It has the form

$$n(t) = \frac{n(0)}{1 - n(0)kt}$$

where $n(0)$ is the maximum amplitude of the oscillations and k is the rate constant. This model was fit to the measurements taken at all

temperatures (See Figures 4.3, 4.4) which determined the rate k as a function of temperature.

4.3.3 Activation Energy

The activation energy should obey the relationship

$$k \propto e^{\frac{-E_a}{k_B T}}$$

where k is the rate from the non-geminate model, k_B is the Boltzmann constant, and T is the temperature. Rearranging this equation gives

$$\ln k \propto \frac{-E_a}{k_B T}$$

where the activation energy can be found as the slope of $\ln k$ versus $1/k_B T$. Figure 4.5 shows that the rate is fairly constant in the temperature range from 240-280 K. In the range from 280-330 K, the logarithm of the rate increases linearly with the inverse of the temperature. It is not entirely clear why this linear behavior does not occur in the lower temperature range. It could be that this method of determining the rate fails at temperatures close to the onset of metastability. A straight line can be fit to the data in the higher temperature range, and the slope of this line gives an activation energy of .784 +/- 0.1 eV.

Similar analysis using an exponential model gave an activation energy of about 0.380 eV.

FIG 4.3 Decay of shallow center at 293 K

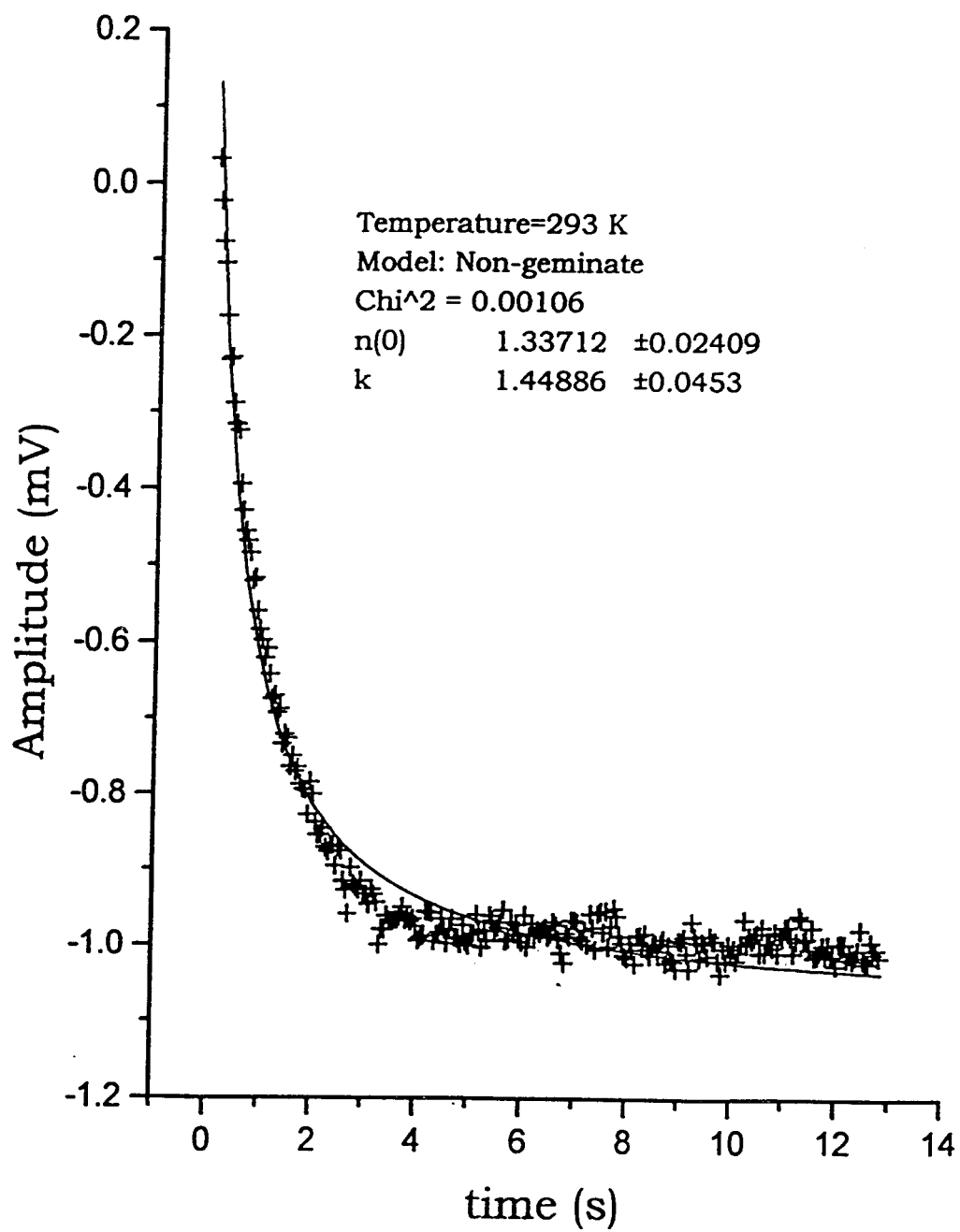


FIG 4.4 Decay of shallow center at 308 K

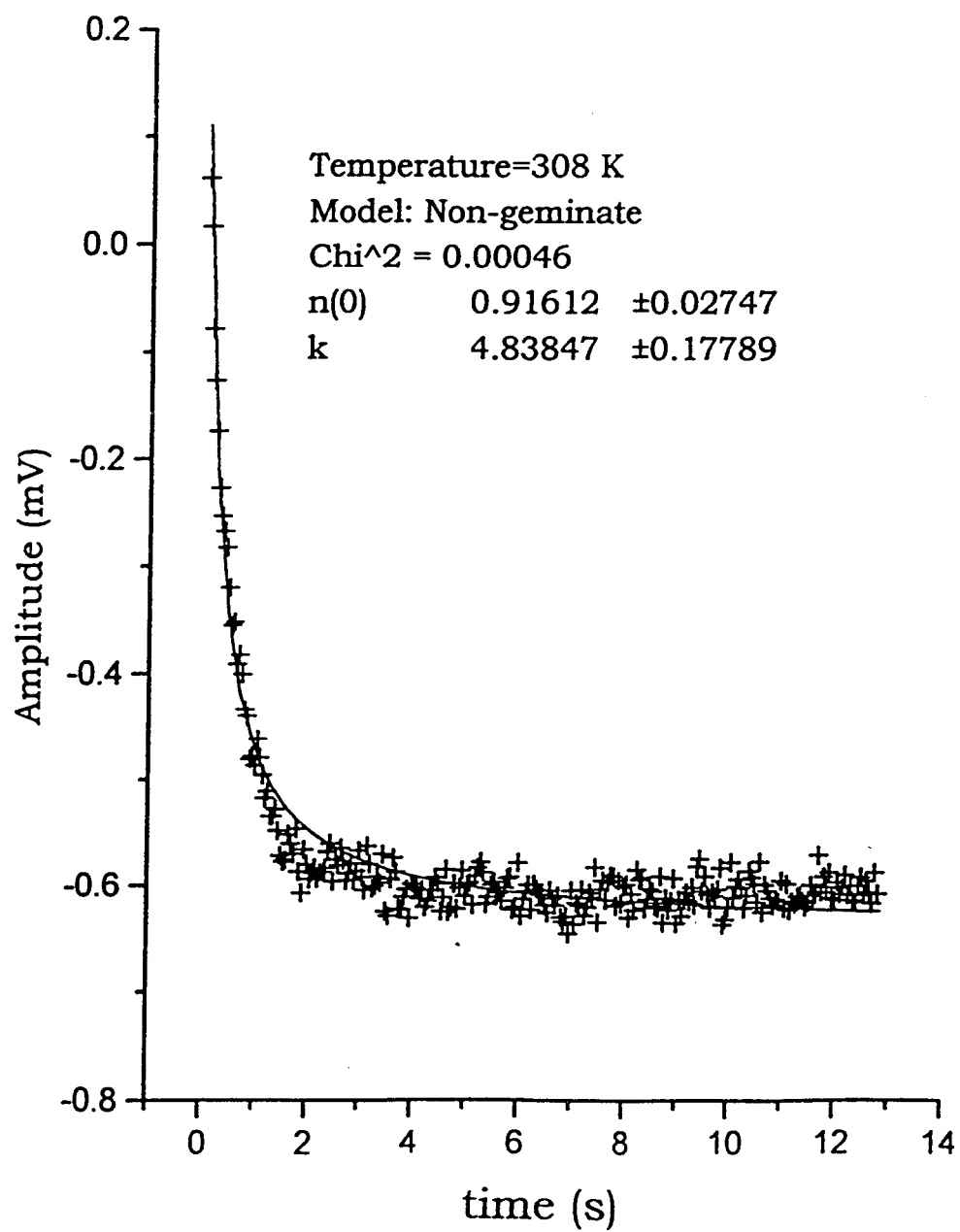
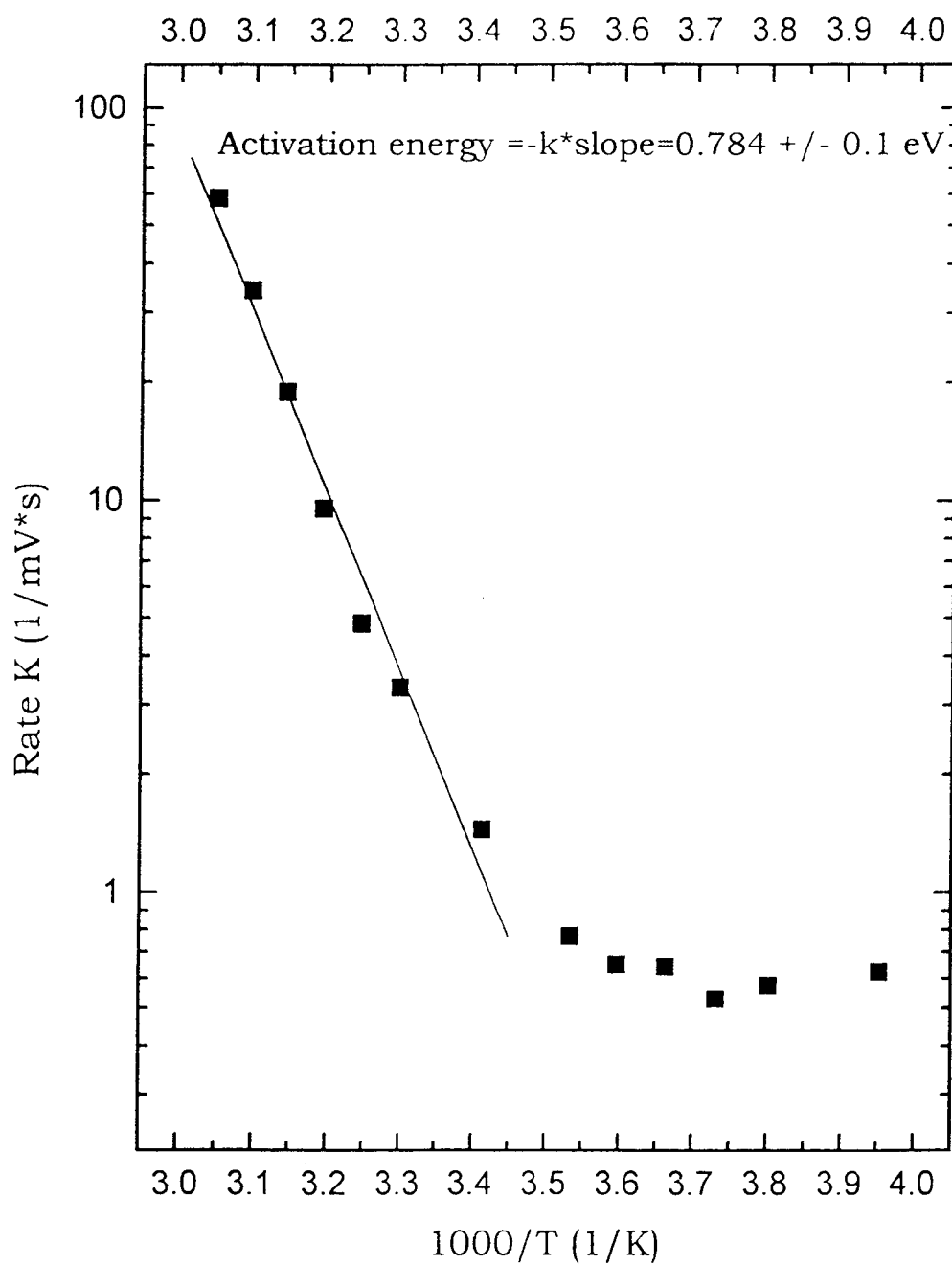


FIG 4.5 Activation energy



5. CONCLUSIONS

This work describes the decay of the shallow center in Ga-doped CdF_2 . Gallium takes the place of cadmium in the host lattice, and forms bistable centers. Due to this bistability, $\text{CdF}_2\text{:Ga}$ undergoes a change in the index of refraction under illumination. This effect makes it possible to write holographic patterns into the crystal.

In this experiment, a holographic grating was written into the sample. The efficiency of the grating is dependent on both the temperature and the intensity of the writing beam. Grating efficiency is a maximum at 285 K, and becomes very small for temperatures below 240 K. This temperature is near the onset of metastability, so the technique used in this experiment is not effective for such low temperatures. The decay of the shallow center was recorded and analyzed for temperatures between 240 and 328 K.

The decay of the shallow center was characterized in two ways. In the first, the decay was fit to a non-geminate recombination model. Using this analysis, the height of the energy barrier between the deep and shallow centers is found to be ~ 780 meV. In the second method, the decay was fit to an exponential model, which gave an activation energy of ~ 380 meV.

The activation energy obtained using the exponential fit is too small to be physically reasonable. The thermal energy barrier between centers is 200 meV in $\text{CdF}_2\text{:In}$, and the temperature for metastability in In-doped crystals is two to three times smaller than that of the Ga-doped crystals[1]. For this to occur, the height of the energy barrier must be considerably higher in the Ga-doped material. It should also be noted that the optical ionization energy for Ga-doped material is also two to three times that of the In-doped material [2]. From this analysis, it seems clear that the activation energy should be higher than the 0.38 eV found from the exponential model. On the other hand, the analysis done using the non-geminate recombination model gives an activation energy several times that of the In-doped crystal. It is very close to the previously determined experimental value of 0.65 eV [1, 11] that was calculated using a different analysis. Both of these experimental values are close to the theoretically predicted value of 1 eV [2]. The energy found in this experiment is within 25% of the theoretical prediction. It seems likely that the decay of the shallow center really is a two-center process, and that the theoretical model may be correct.

BIBLIOGRAPHY

1. A. Suchocki, B. Koziarska, T. Langer, J.M. Langer, "Room-temperature holographic grating recording in $\text{CdF}_2\text{:Ga}$ ", Appl. Phys. Lett. **70**, 2934-2936, (1997).
2. C.H. Park, D.J. Chadi, "First-Principles Study of Structural Bistability in Ga-and In-Doped CdF_2 ", Phys. Rev. Let. **82**, 113-116, (1998).
3. A. Suchocki, J. Rauluszkiewicz, J.M. Langer, "Photoinduced metastable lattice dilation in $\text{CdF}_2\text{:In}$ crystals", Appl. Phys. Lett. **71**, 1552-1554, (1997).
4. J.M. Langer, A. Suchocki, R. Szymczak, M. Baran, "Photoinduced magnetism in CdF_2 with bistable donors: The clue for the negative U?" Mat. Sci. Forum, **258-263**, 1449-1454, (1997).
5. A.I. Ryskin, P.P. Fedorov, "Donor impurities and DX centers in the ionic semiconductor CdF_2 ", Phys. Solid State **39**, 943-947, (1997).
6. S.A. Kazanskii, A.I. Ryskin, V.V. Romanov, "Paramagnetic susceptibility of semiconducting $\text{CdF}_2\text{:In}$: Direct evidence of the negative-U nature of the DX-like center", Appl. Phys. Lett. **70**, 1272-1274, (1997).
7. Z. Wilamowski, J. Dmochowski, W. Jantsch, "EPR investigation of metastable donor states in $\text{CdF}_2\text{:In, Ga}$ ", Mat. Sci. Forum, **258-263**, 1443-1448, (1997).
8. A.S. Shcheulin, A.I. Ryskin, K. Swiatek, J.M. Langer, "Deep-shallow transformation of bistable centers in semiconducting CdF_2 crystals", Phys. Let. A, **222**, 107-112, (1996).
9. J. Dmochowski, J. Langer, Z. Kalinski, W. Jantsch, " $\text{CdF}_2\text{:In}$ —A Critical Positive Test of the Toyozawa Model of Impurity Self-Trapping", Phys. Rev. Let., **56**, 1735-1737, (1986).
10. J. Nissila *et al.*, "Universality of the Bond-Breaking Mechanisms in Defect Bistability: Observation of Open Volume in the Deep States of In and Ga in CdF_2 ", Phys. Rev. Let., **82**, 3276-3279, (1999).

11. A.I. Ryskin *et. al.*, "Mechanisms of writing and decay of holographic gratings in semiconducting $\text{CdF}_2\text{:Ga}$ ", J. of Appl. Phys., **83**, 2215- 2221, (1998).
12. A.I. Ryskin, A.S. Shcheulin, D.E. Onopko, "DX Centers in Ionic Semiconductor $\text{CdF}_2\text{:Ga}$ ", Phys. Rev. Let., **80**, 2949-2952, (1998).
13. W. Warren, Jr., B.F. Campbell, G.F. Brennert, "Picosecond Recombination Dynamics of Electrons in Ionic Liquids", Phys. Rev. Let. **58**, 941-943, (1986).
14. Cryogenic Microminiature Refrigeration System IIB, Model K2205, MMR Technologies, Inc., Mountain View, CA.
15. E. Hecht, *Optics*, Second Edition, Addison-Wesley Publishing Co., Massachusetts, 1987.
16. A.I Ryskin, A.S. Shcheuling, D.E. Onopko, "DX Centers in Ionic Semiconductor $\text{CdF}_2\text{:Ga}$ ", Phys. Rev. Let., **80**, 2949-2952, (1997).